Influence of infill pattern and layer height on additively manufactured 17-4 PH/PLA composite

Fredrick Mwema[1*], *Job* Wambua[2], *Stephen* Akinlabi[2], *Tien-Chien* Jen[1], and *Esther* Akinlabi[2]

[1]Department of Mechanical Engineering Science, University of Johannesburg, APK Campus, South Africa
[2]Department of Mechanical & Construction Engineering, Northumbria University, NE1 8ST Newcastle, United Kingdom

Abstract. Additive manufacturing or 3D printing of components is now becoming a very attractive method of producing models and parts in the medical, automotive, aerospace, and clothing industries, among many others. Despite the numerous advantages associated with 3D printing of components, the uptake of this technology is still in the early stages, owing to the limited research and data availability on the process, safety of components, and their integrity. Material extrusion 3D printing process is currently being investigated for manufacturing of metal composites and is one of the interesting subjects in fused deposition modelling. This study investigates the effect of infill pattern (lines, gyroid, cross, and lines) and layer height (0.15 mm, 0.1 mm, and 0.2 mm) on the dimensional deviation and mechanical properties of 3D printed 17-4 PH/PLA composites. The samples were produced through fused deposition modelling and evaluated for dimensional stability and tensile properties. In terms of dimensional accuracy, it is observed that for all samples, the width had the highest accuracy, followed by the height and finally the length. The largest width errors were observed for samples prepared at a layer height of 0.15 mm and gyroid infill patterns. The smallest width errors were observed on samples fabricated at a layer height of 0.2 mm and lines infill pattern. As expected, 3D printing at the lowest layer height of 0.1 mm resulted in the minimum dimensional error of the length of these samples. The lowest mechanical strength was reported at samples fabricated at an infill pattern of lines and layer heights of 0.1 mm and 0.2 mm.

1 Introduction

Additive manufacturing (AM) technologies have evolved and are gaining popularity for potential applications in areas such aerospace, automotive, energy, water, and biomedical sectors. Fused Filament Fabrication (FFF) or material extrusion additive manufacturing is one of the most popular AM methods for processing of polymer materials. Due to affordability and availability of desktop FFF printers (commonly known as fused deposition

* Corresponding author: fredrick.mwema@northumbria.a.c.uk

modelling, FDM, printers), the technique has been extensively evaluated for a wide range of materials with great success on polymeric materials [1]. The most interesting aspect of FDM (and the rest of the 3D printing methods) is the capability to produce intricate shapes and structures. As such, it can be used to manufacture complex engineering structures for different applications.

The influence of various processing parameters of FDM on the properties of the manufactured parts has been extensively explored by various researchers. These parameters include temperature, speed, resolution, layer height, infill density, infill pattern, and build orientation, among others [2]. The fabrication of metal parts through FDM is gaining interest among researchers and it has been demonstrated that the feasible approach is to use a metal-polymer composite to undertake the process. Several studies are reporting on this subject, and it is generally shown that the printed parts must undergo thermal processes to extract the polymeric components and stabilize the metallic part [3, 4]. Several studies are being undertaken on this subject and various aspects of processing have been published [5-8]. To contribute to the ongoing efforts, this article reports on the effect of infill pattern and layer height on the dimensional and mechanical properties of a 3D printed 17-4 PH/PLA composite.

2 Methods

The filament material used in this study (17-4 PH/PLA composite) was sourced from BASF, UK. The samples were prepared using the Ultimaker S5 3D printing machine (Utrecht, Netherlands) according to the BASF recommended printer settings for the 17-4 PH PLA composite: core type CC (0.4 mm), nozzle temperature of 240oC, build plate temperature of 70oC, infill density of 105%, and a normal printing resolution of 0.15 mm. The recommended settings for the infill pattern and layer height, as provided by BASF are lines and 0.15 mm, respectively. The values and parameters adopted in this work are displayed in Table 1.

Table 1. Printing parameters and the design of experiments

Exp. No.	Infill pattern	Layer height (mm)
S1	Lines	0.15
S2	Gyroid	0.15
S3	Cross	0.15
S4	Lines	0.1
S5	Lines	0.2

The five samples were designed as rectangular bars of 5 mm × 3 mm × 50 mm using Autodesk Inventor 2023 (student version) to meet the requirements of the ASTM D3039 standard. They were then sliced using Ultimaker Cura (open-source software) and then exported for 3D printing. After printing, the physical dimensions of the samples were measured using a vernier calliper. For every condition, three samples were printed. The surfaces of the printed composites were examined using a confocal laser scanning microscope (Olympus LEXT OLS5100, Evident, UK). The tensile tests were conducted using a floor model universal testing machine (100 kN Instron 3382, Boston, USA) at a constant crosshead speed of 2 mm/min (0.05 in/min) as per the ASTM D3039 standard [9]. The fractured surfaces of the samples were imaged using a Digital Microscope (Dino-Lite AM4115ZT, RS Components) at a magnification of X1600 [10].

3 Results and Discussion

The 3D printed 17-4PH/PLA composites were observed using a confocal laser scanning microscope (CLSM) on the parallel and normal surfaces to the Z-direction. On the surfaces parallel to the Z-orientation, the 3D printing layer lines were observed (Figure 1). These layers appeared as distinct boundaries and were more visible in S5 and S3 (Figure 1). The surfaces of S4 appeared smoother and the layer lines were less visible. These observations were further confirmed via topography imaging (Figure 2). These images are significant in revealing the quality of adhesion between adjacent layers of PLA and 17-4PH stainless steel after extrusion. As such, S5 and S3 in which clear boundaries across the layers can be seen are indications of poor adhesion among the layers. The CLSM images were also taken on the surface normal to the printing direction (Figure 3). As expected, the dual-phase structure of the composite is visible. The images on this surface provide information about the homogeneity of the printed materials; there is better distribution/filling of the extruded composite materials in S1, S2, and S4. The presence of printing tracks on samples S3 and S5 leads to non-uniformity. These images also reveal surface deformities such as voids, cracks, and surface irregularities in samples S5, S4 and S3. The roughness values (Sa) of these surfaces were computed based on Figure 4 as S1 = 8.74 μm, S2 = 28.20 μm, S3 = 11.23 μm, S4 = 7.20 μm, and S5 = 13.72 μm. These results demonstrate that the gyroid infill pattern results in very high roughness for PLA/17-4PH stainless steel composites. For the line infill pattern, the Sa increases with the layer height, hence the high roughness in S5.

To further evaluate the printing quality of the 17-4PH/PLA composite, dimensional deviations of the printed samples from the design were evaluated. Three measurements (length, width, and height) of the printed samples were obtained on all three sides and then averaged for each to obtain the actual print dimensions as provided in Table 2. The percentage changes in the dimensions in comparison to the design dimensions are also shown in Table 2. It was observed that on printing, the actual print dimensions increased by a significant value more than the anticipated change of 5% from the recommended print setting of the infill density (105%). The largest percentage change (of more than 21%) was observed in the width, which was the direction of the printing (z-axis). This could have been attributed to the small deviations in the layer heights as the printing progressed in the z-direction. Sample S2 (gyroid infill density and layer height of 0.15 mm) experienced the largest deviation in its width. The deviations in dimensions could be attributed to the irregularities and extrusion inconsistencies observed via the CLSM images.

On undertaking the tensile testing (Figure 5), the failure of the samples occurred at various sections of the samples, which is different from the traditional tensile tests in which fracture occurs at the central region of the sample, which can be related to the printing defects of the samples. As noted, CLSM images on the surface of the samples (Figure 3) indicated irregularities such as layer lines, separation between the layers, and voids. There were also extrusion inconsistencies, incomplete infill, and misalignments in S2, S4, and S5 (Figure 3). Tensile tests conducted on the 3D-printed samples yielded the force-displacement results presented in Figures 6 and 7. As shown, the load-displacement behaviour is dependent on the infill pattern and layer height. The maximum force in the curve determines the load the material can withstand without failure; and in this case, S1 can withstand the highest maximum force (about 181 N) followed by S3 (180 N) and S2 (179.5 N). Samples S1, S3 and S2 were printed at the lower layer height of 0.15 mm, which means that lower layer height enhances the loading capacity of the printed 17-4/PLA composite [11, 12]. Additionally, the sample prepared with the infill pattern of lines (S1) exhibited the highest loading capabilities as compared to cross (S3) and gyroid (S2) infill patterns [13]. Sample S1

exhibits uniform morphology and topography (Figures 3 and 4) with the least defects on the printed surface. The gyroid structured printed parts (S2) were seen to exhibit high loading capability despite exhibiting the highest roughness. Samples S4 and S5 prepared using an infill pattern of lines and the highest layer heights of 0.1 mm and 0.2 mm, respectively, exhibit the lowest loading capacities. This is because the overlap between adjacent infill lines may lead to gaps in the infill pattern that act as sites for crack initiation and growth, leading to the eventual failure of the print.

Upon examination of the fracture surfaces (Figure 8), it was observed that S1 had some cracks at 45° (circled with the discontinuous line in Figure 8) in addition to voids/spaces which could have been responsible for the fracture in uniaxial loading. In S2, there were cracks (as shown in Figure 8) parallel to the direction of material extrusion during the printing process. In this sample, there were no clear voids on the fracture surface. In S3, the fracture surfaces showed lumps of extruded material, which could be attributed to the nature of the infill pattern (cross) and act as stress raisers and hence sites for crack initiation. There were also voids observed around these lumps, which could also be responsible for uniaxial failure. The fracture surface in S4 revealed a dense morphology with pit-like voids distributed all over the surface. Additionally, the surface revealed misalignment of the morphology in some areas (circled with the discontinuous line in Figure 8), which could be attributed to premature solidification and hence non-uniform morphology alignment. The fracture surface of S5 revealed many voids on adjacent layers, which could have been the reason for the low loading capacity of the samples. The low resolution (0.2 mm) results in poor layer adhesion and low mechanical strength [14]. These observations indicate that infill pattern and layer height influence the tensile properties of 17-4PH/PLA composites fabricated via fused deposition modelling; these findings are consistent with published literature [15].

Table 2. Dimensions of the 17-4PH/PLA composite on 3D printing (Design dimensions: 5 mm × 3 mm× 50 mm)

Sample	**Actual Print Dimensions**												**% error in dimensions**		
	L (mm)				W (mm)				H (mm)						
	1	2	3	Avg	1	2	3	Avg	1	2	3	Avg	%ΔL	%ΔW	%ΔH
S1	5.95	5.93	5.90	**5.93**	3.67	3.70	3.67	**3.68**	59.95	59.70	59.61	**59.75**	**18.6**	**22.6**	**19.5**
S2	5.93	5.92	5.91	**5.92**	3.69	3.70	3.72	**3.70**	59.65	59.74	59.65	**59.68**	**18.4**	**23.3**	**19.4**
S3	5.97	5.98	5.99	**5.98**	3.65	3.63	3.64	**3.64**	59.50	59.74	59.63	**59.62**	**19.6**	**21.3**	**19.2**
S4	5.88	5.94	5.86	**5.89**	3.65	3.67	3.65	**3.66**	59.65	59.66	59.63	**59.65**	**17.8**	**22.0**	**19.3**
S5	6.02	5.98	5.99	**6.00**	3.63	3.62	3.63	**3.63**	59.70	59.71	59.72	**59.71**	**20.0**	**21.0**	**19.4**

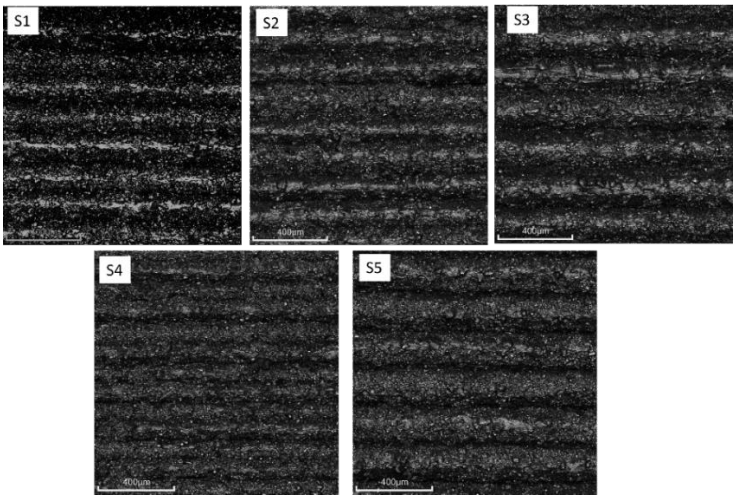

Fig. 1. CLSM images taken on surfaces parallel to the printing direction (Z-direction) of the 17-4PH/PLA composites.

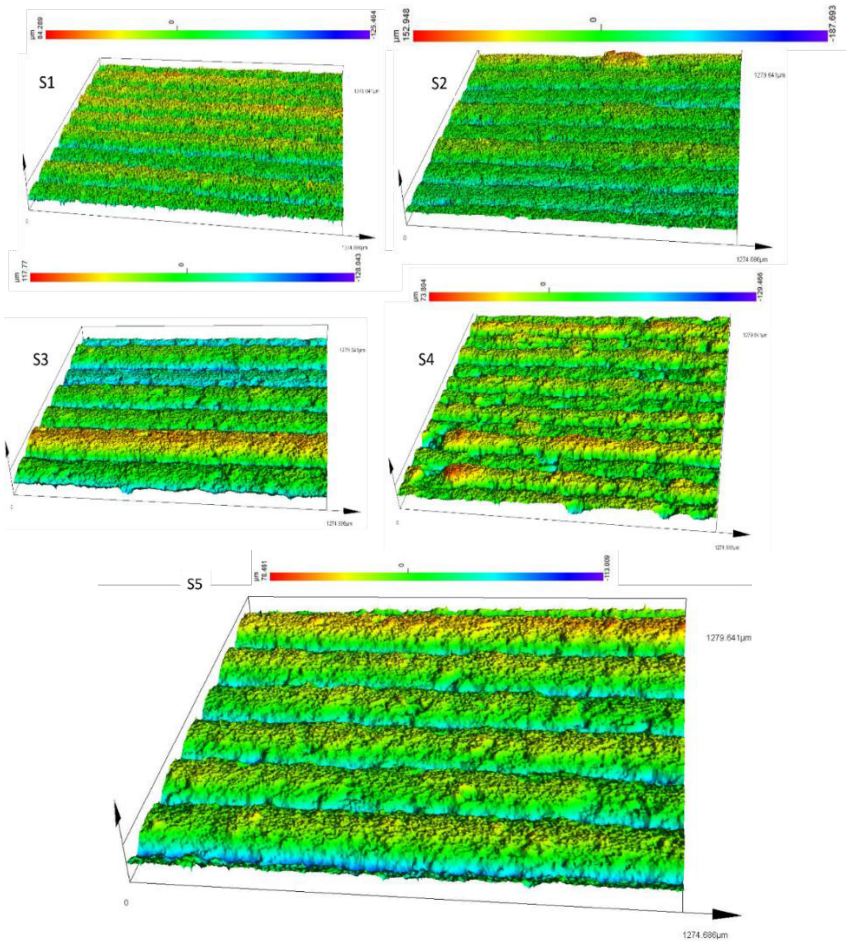

Fig. 2. Topography of the surfaces parallel to the printing direction (Z-direction) of the 17-4PH/PLA composites obtained using CLSM.

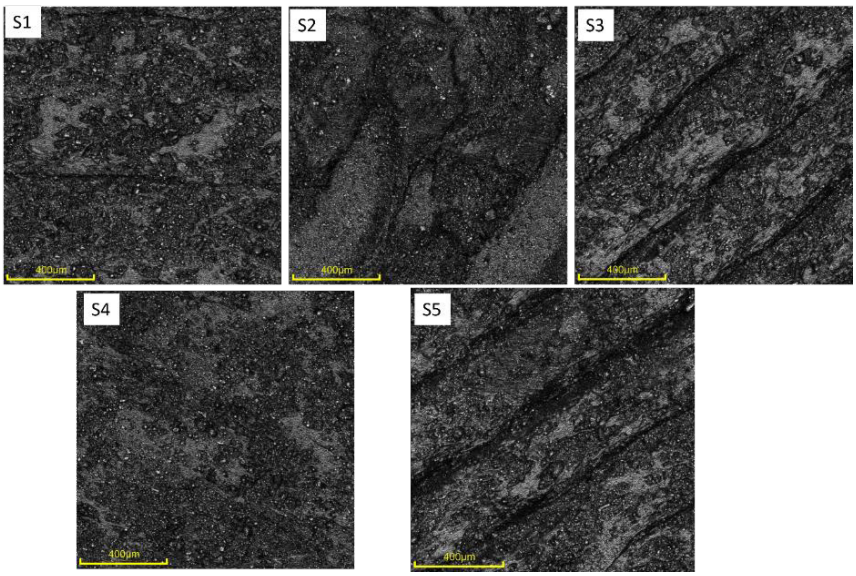

Fig. 3. CLSM images taken on surfaces perpendicular to the printing direction (Z-direction) of the 17-4PH/PLA composites.

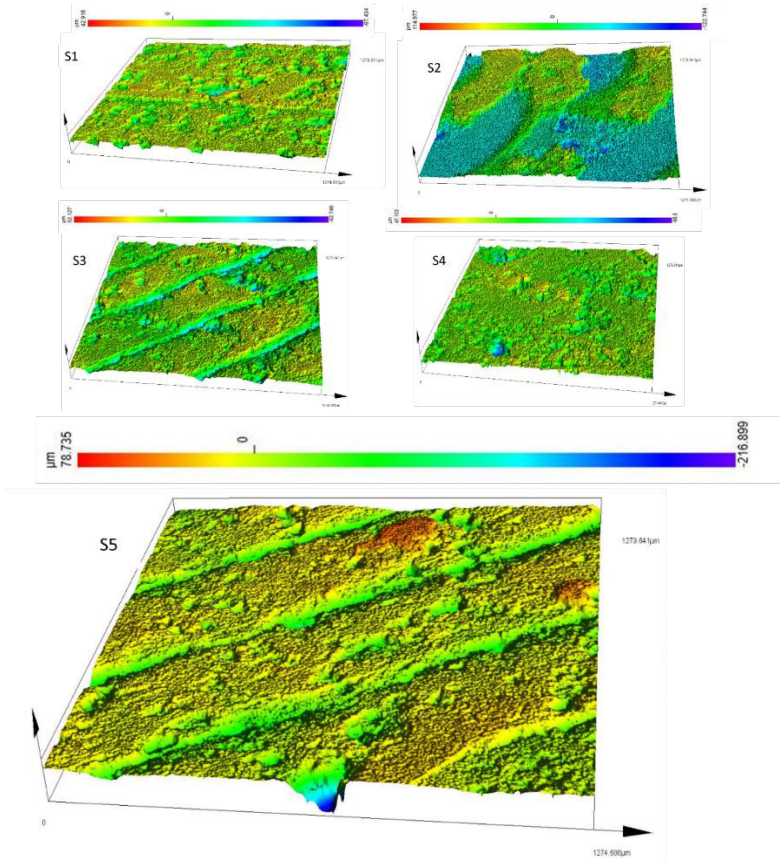

Fig. 4. Topography of the surfaces perpendicular to the printing direction (Z-direction) of the 17-4PH/PLA composites obtained using CLSM.

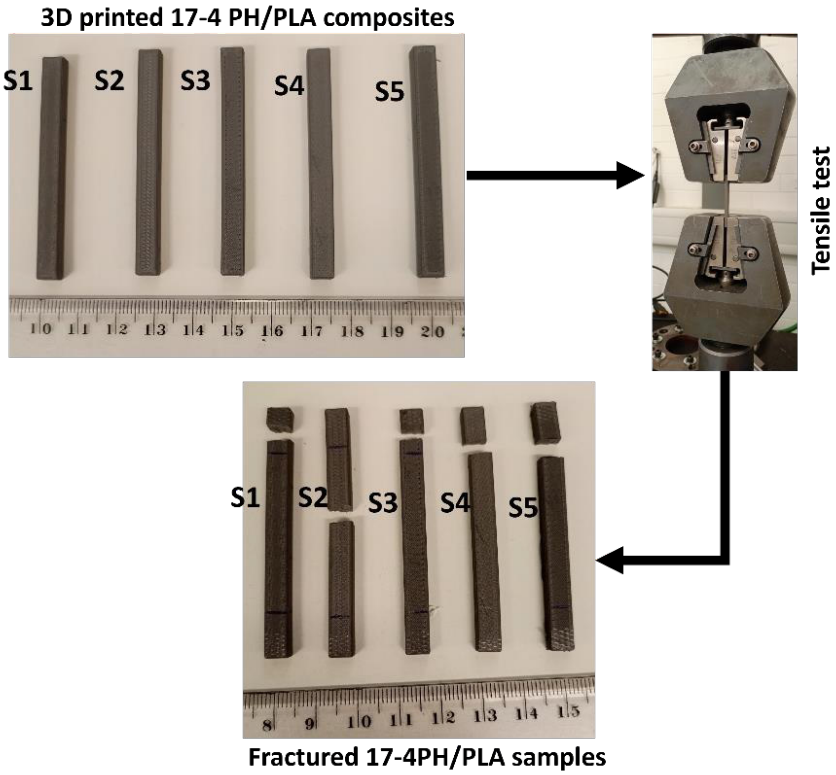

Fig. 5. A picture of the 3D-printed 17-4PH/PLA composite before and after tensile testing

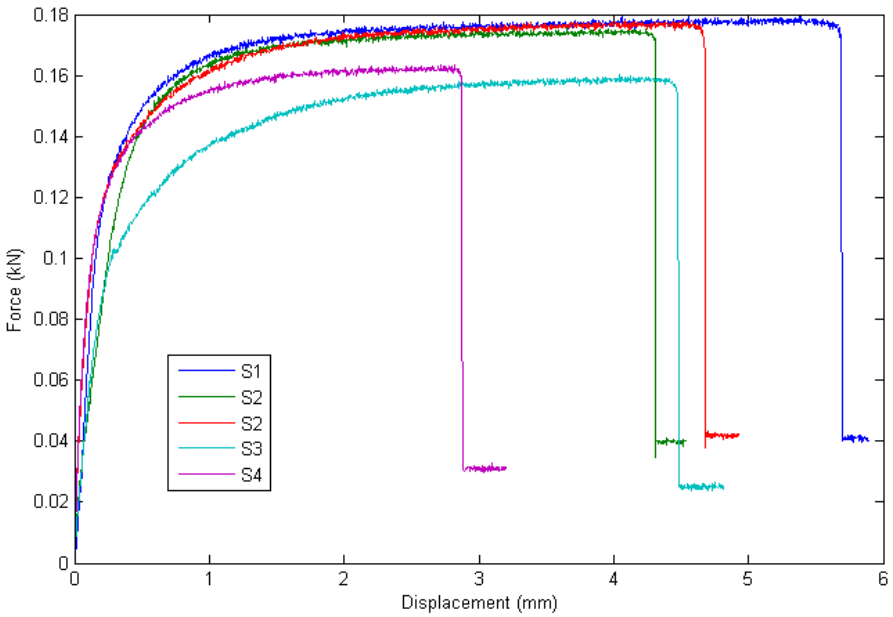

Fig. 6. Force against displacement plots for the samples during the tensile tests.

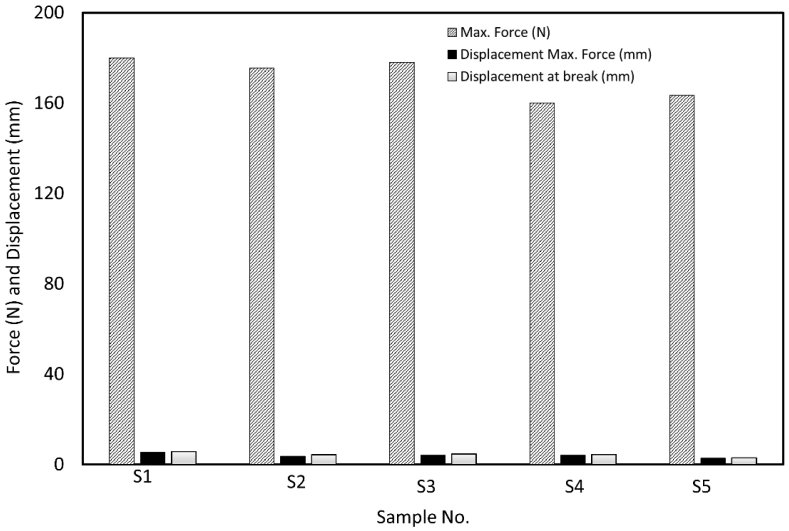

Fig. 7. Tensile properties of the 3D printed 17-4PH/PLA composite samples.

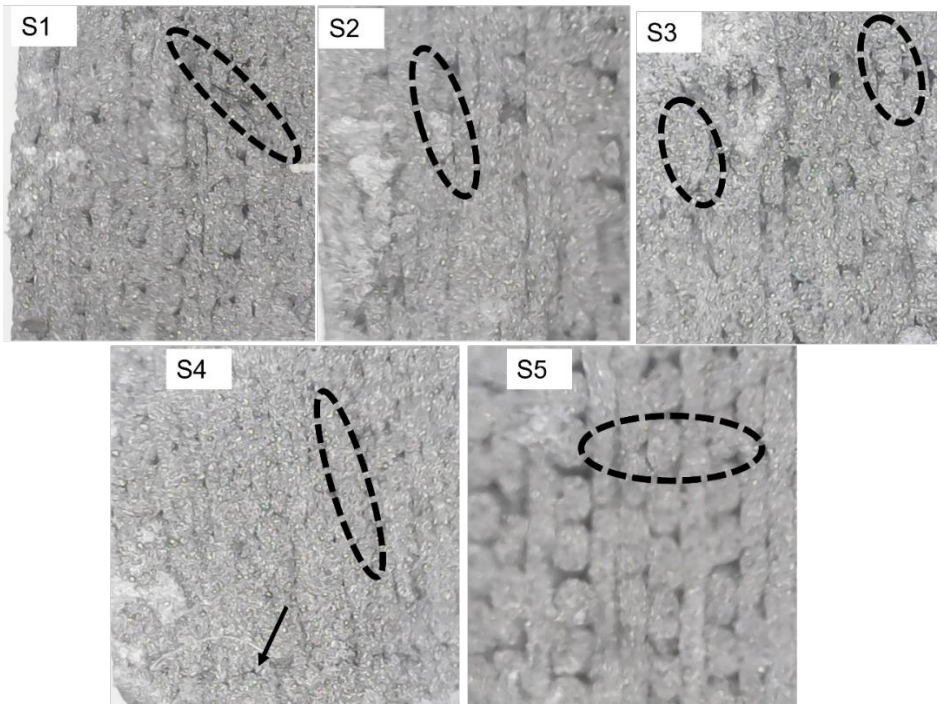

Fig. 8. Fracture surfaces of the 3D printed 17-4PH/PLA composites. The images were taken at a magnification of x1600.

4 Conclusions

In this article, the influence of infill pattern and layer height on the quality and strength of 3D printing of 17-4PH/PLA composite is reported. The composite was printed through material extrusion additive manufacturing (fused deposition modelling) and then evaluated for dimensional accuracy, structural

integrity, and mechanical loading. The surface roughness of the 3D printed composites is influenced by the infill pattern and layer height in that the higher the layer height, the lower the surface roughness. Gyroid infill pattern produces samples with very high surface roughness. The dimensional variation of the printing of 17-4PH/PLA composite is influenced by both the infill pattern and the layer height. The microstructure of the composite and the occurrence of defects depends on the layer height as demonstrated in the topography and fracture surface analysis. The mechanical strength is also shown to depend on these parameters of the 3D printing process and usually the fracture occurs due to presence of defects such as cracks, voids, lumped, and misaligned layers. Samples printed at a moderate/normal layer height of 0.15 mm support the highest loads which also vary with the infill pattern with lines exhibiting the highest.

References

1. F. M. Mwema and E. T. Akinlabi, Basics of Fused Deposition Modelling (FDM), in Fused Deposition Modeling: Strategies for Quality Enhancement, F. M. Mwema and E. T. Akinlabi Eds. Cham: Springer International Publishing, 2020, pp. 1-15.
2. H. Cheng et al., Effects of rCF attributes and FDM-3D printing parameters on the mechanical properties of rCFRP. Composites Part B: Engineering. **270**, 111122 (2024). https://doi.org/10.1016/j.compositesb.2023.111122
3. Z. Liu, Q. Lei, S. Xing, Mechanical characteristics of wood, ceramic, metal, and carbon fibre-based PLA composites fabricated by FDM. Journal of Materials Research and Technology, **8,** 5, 3741 (2019). https://doi.org/10.1016/j.jmrt.2019.06.034
4. Y.-H. Cho, S.-Y. Park, J.-Y. Kim, K.-A. Lee, 17-4PH stainless steel with excellent strength–elongation combination developed via material extrusion additive manufacturing. Journal of Materials Research and Technology, **24**, 3284 (2023) https://doi.org/10.1016/j.jmrt.2023.03.228
5. J. Mogan et al., Thermo-mechanical properties of ABS/stainless steel composite using FDM. Materials Today: Proceedings, (2024). https://doi.org/10.1016/j.matpr.2024.01.029
6. R. Kumaresan et al., Preliminary investigation on the tensile properties of FDM printed PLA/ copper composite. Materials Today: Proceedings, (2023). https://doi.org/10.1016/j.matpr.2023.10.054
7. H. Ramazani, A. Kami, Metal FDM, a new extrusion-based additive manufacturing technology for manufacturing of metallic parts: a review. Progress in Additive Manufacturing, **7**, 4, 609 (2022). https://doi.org/10.1007/s40964-021-00250-x
8. K. Rane, M. Strano, A comprehensive review of extrusion-based additive manufacturing processes for rapid production of metallic and ceramic parts. Advances in Manufacturing, **7**, 2, 155 (2019). https://doi.org/10.1007/s40436-019-00253-6
9. S. Rodrigues et al., Towards optimization of polymer filament tensile test for material extrusion additive manufacturing process. Journal of Materials Research and Technology, **24**, 8458 (2023). https://doi.org/10.1016/j.jmrt.2023.05.088
10. M. A. Muflikhun, T. Yokozeki, Systematic analysis of fractured specimens of composite laminates: Different perspectives between tensile, flexural, Mode I, and Mode II test. International Journal of Lightweight Materials and Manufacture, **6**, 329 (2023). https://doi.org/10.1016/j.ijlmm.2023.03.003
11. K. Almansoori, S. Pervaiz. Effect of layer height, print speed and cell geometry on mechanical properties of marble PLA-based 3D printed parts. Smart Materials in Manufacturing, **1**, 100023 (2023). https://doi.org/10.1016/j.smmf.2023.100023

12. J. R. Stojković et al., An Experimental Study on the Impact of Layer Height and Annealing Parameters on the Tensile Strength and Dimensional Accuracy of FDM 3D Printed Parts. Materials, **16**, 13, (2023). https://www.mdpi.com/1996-1944/16/13/4574
13. M. Ö. Öteyaka, F. H. Çakir, M. A. Sofuoğlu, Effect of infill pattern and ratio on the flexural and vibration damping characteristics of FDM printed PLA specimens. Mater Today Commun, **33**, (2022). https://doi.org/10.1016/j.mtcomm.2022.104912
14. S. Song, J. Zhang, M. Liu, F. Li, S. Bai, Effect of build orientation and layer thickness on manufacturing accuracy, printing time, and material consumption of 3D printed complete denture bases. Journal of Dentistry, **130**, 104435 (2023). https://doi.org/10.1016/j.jdent.2023.104435
15. T. Yao, J. Ye, Z. Deng, K. Zhang, Y. Ma, H. Ouyang, Tensile failure strength and separation angle of FDM 3D printing PLA material: Experimental and theoretical analyses. Composites Part B: Engineering, **188**, 107894 (2020). https://doi.org/10.1016/j.compositesb.2020.107894